

Original article

The impact of background water flow on the early migration of a CO₂ plume in a tilted aquifer during the post-injection period

Mawda Awag^{✉*}, Eric Mackay, Saeed Ghanbari

Institute of GeoEnergy Engineering, Heriot-Watt University, Edinburgh EH14 4AS, United Kingdom

Keywords:

CO₂ plume migration
background flow velocity
tilted aquifer
plume distribution
migration distance

Cited as:

Awag, M., Mackay, E., Ghanbari, A. The impact of background water flow on the early migration of a CO₂ plume in a tilted aquifer during the post-injection period. *Advances in Geo-Energy Research*, 2023, 9(2): 125-135.
<https://doi.org/10.46690/ager.2023.08.06>

Abstract:

The study presents a numerical modelling analysis on CO₂ plume migration in a dipping storage aquifer with background flux, which incorporates residual and dissolution trapping of CO₂. The purpose of this analysis is to investigate the effect of the background flow velocity on the CO₂ plume migration during the early post-injection period. Different velocities of groundwater flow from low to high were considered in the aquifer model. The distribution, migration distance and velocity of the injected CO₂ plume as well as the remaining mobile CO₂ plume extent are estimated to determine how fast and far the plume propagates with time. Comparison of the results indicate that increasing the background flux velocity causes the plume to migrate longer distances up-dip, while it reduces the height distribution of the plume with time. This reduces the volume of mobile CO₂ in the storage aquifer at larger velocities of background flux, hence decreasing the leakage risk of CO₂ to the surface. In addition, the CO₂ plume decelerates immediately after cessation of injection as its bottom rises vertically and the buoyancy force reduces as the thickness of the plume reduces. However, the plume then accelerates during the initial period of its subsequent lateral migration, as the plume becomes extended, and the buoyancy forces increases somewhat. The degree of lateral extension increases with increasing background water flow velocity, with the leading tip of the plume migrating faster than the trailing edge, until residual and dissolution trapping sufficiently reduce the volume of free phase CO₂ that its migration is arrested.

1. Introduction

The reduction of global atmospheric Carbon Dioxide (CO₂) emissions is essential to diminish climate change. CO₂ injection into deep saline aquifers is the most assuring method for long-term storage of CO₂, due to their large potential storage capacities as well as their wide availability around the globe (Birkholzer et al., 2015). Saline aquifers offer global storage capacities from 4,000 to 23,000 Gigatons of CO₂, which make them suitable repositories for permanently storing the CO₂ captured from anthropogenic sources (Bennaceur, 2014). Their depths range from 1,000 to 3,000 meters underneath the surface, which provide the required environment for the CO₂ to remain under supercritical

conditions. They are generally thin and can be horizontal or tilted (Rosenbauer and Thomas, 2010).

Under typical aquifer conditions, the density and viscosity of the CO₂ plume are always less than those of resident formation brine, which make the CO₂ more mobile (Pruess and Nordbotten, 2011). In the absence of barriers to vertical flow, the injected plume of CO₂ migrates upwards until reaching a low permeability caprock, and then it spreads laterally while migrating for several years because of the buoyancy effect and background flow velocity (Elenius et al., 2015). This increases the possibility of CO₂ leakage through spill points, including faults or fractures and abandoned wells. Thus, ensuring that the injected CO₂ becomes trapped within the target formation it is injected into is important for long-term storage.

Leakage of the injected plume of CO₂ back to the surface is prevented via four main trapping processes: (1) Structural trapping in which the injected plume of CO₂ becomes trapped under an impermeable caprock while remaining mobile (Riaz and Cinar, 2014); (2) Residual trapping occurs after injection ceases when the CO₂ at the trailing end of the plume is immobilised as water is imbibed behind it (Pentland et al., 2011); (3) Dissolution trapping happens over a long timescale, in which the mobile and residual CO₂ dissolve slowly into the brine (Iglauer, 2011). CO₂ dissolution offers greater storage security, since the CO₂ saturated brine is much denser than the unsaturated brine, and thus the dissolved CO₂ is displaced downwards away from the interface (Zhang and Song, 2014). (4) mineral trapping takes place when the dissolved CO₂ reacts with the rock, precipitating carbonate minerals; however, this does not impact the plume migration as it occurs only after the CO₂ has dissolved into the brine (Gunter et al., 1997; Oelkers, 2008). The fate of the injected plume of CO₂ in an open storage aquifer is a function of these mechanisms, and they establish what volume of CO₂ remains mobile during migration (Pawar et al., 2020).

During the injection of CO₂, the overall CO₂ saturation increases as the leading tip of the plume displaces brine and no residually trapped CO₂ is yet formed at the trailing edge of the plume (IPCC, 2005). Once injection ceases, the injected CO₂ plume may migrate for hundreds to thousands of years, and residual CO₂ as well as dissolved CO₂ are trapped in the wake of the injected CO₂ plume (Benson and Cole, 2008). Therefore, a complete understanding of the subsurface spreading and trapping of the injected CO₂ plume is vital to estimate the storage capacity as well as security (Bachu, 2008). Various analytical and numerical studies explored different aspects of CO₂ storage and migration in deep saline aquifers. Most of these studies assumed that the aquifer brine is stagnant, where in fact many aquifers are exposed to a slow groundwater flow. For example the flow velocity of the groundwater (Darcy velocity) in deep aquifers in the Alberta Basin is 1 to 10 cm/year (Bachu et al., 1994; Han et al., 2011). In addition, strata in the majority of aquifers are tilted and this can affect the movement of underground water, which in turn can impact the CO₂ migration behaviour in storage aquifers.

Among previous studies, Nordbotten et al. (2005) analysed analytically the shape of an injected plume of CO₂ into an aquifer during the injection period and provided a solution for the problem where viscous forces dominate over buoyancy forces in the context of CO₂ leakage. Nordbotten and Celia (2006) then included some dissolution effects in the study and showed a favourable comparison of their analytical solution with numerical results. However, residual trapping of CO₂ and groundwater flow effects were not considered in these studies. Hesse et al. (2006) developed a semi-analytical solution for the post-injection migration of an injected CO₂ plume into a confined horizontal aquifer, considering the residual trapping. They gave scaling laws for the volume and extent of an injected CO₂ plume into horizontal aquifers. They used a similar numerical model to Nordbotten et al. (2005) to study the up-dip migration of a CO₂ plume in unconfined tilted aquifers but excluded the CO₂ dissolution in brine and

groundwater movement. Hesse et al. (2007) provided early and late-time similarity solutions for the post-injection migration of CO₂ in a horizontal aquifer without residual or dissolution trapping of CO₂. Hesse et al. (2008) then included the residual trapping effect, showing that the early-period advancement of the plume remains self-similar in a confined horizontal aquifer when residual trapping is incorporated. They also provided scaling laws for the late-period evolution of the plume and presented a solution for confined aquifers when the up-dip migration dominates buoyancy.

Juanes and MacMinn (2008) and Juanes et al. (2009), provided an analytical solution for the CO₂ plume migration in a horizontal aquifer with background water flow when the spreading due to advection caused by groundwater flow dominates the spreading due to buoyancy effects. They considered the preliminary shape of the CO₂ plume during injection and the residual trapping of CO₂, neglecting the dissolution of CO₂ into brine. Their analysis shows that the shape of the CO₂ plume during the injection period has an impact on the evolution of the CO₂ plume. MacMinn and Juanes (2009) performed a similar study for the post-injection migration of an axisymmetric plume of CO₂ in a horizontal aquifer subjected to residual trapping, but with no regional background flow. Their outcomes were comparable to their previous studies. MacMinn et al. (2010) developed a theoretical solution to a hyperbolic gravity-current model for a CO₂ plume migration and residual trapping in a confined dipping storage aquifer subjected to background water flow and accounted for the CO₂ plume shape during injection period as an initial condition for the plume migration during the post-injection period. Their analysis also confirms that the diffusive spreading of the plume due to buoyancy has a trivial impact on the ultimate evolution of the injected CO₂ plume.

Hassanzadeh et al. (2009) and Emami-Meybodi et al. (2015) focused on how the groundwater flux can influence the development of convective mixing during CO₂ dissolution. Hassanzadeh et al. (2009) used a linear stability analysis to derive a time scale for the onset of convective mixing as a function of background flux, to understand the effect of background water flow in aquifers on the onset of convection in a transient concentration field. Emami-Meybodi et al. (2015) studied the effect of groundwater flow on the CO₂ dissolution in brine in saline aquifers considering the diffusion, advection, and convection processes. They developed a semi-analytical model to assess the total dissolution rate and distribution of dissolved CO₂ in the aquifer. They then demonstrated how background flow alters the convective dissolution of the CO₂ in brine using numerical simulations. Their results indicated a delay in the onset of convection and subsequent mixing when groundwater flow exists. Unlike previously mentioned studies, we carried out a numerical modeling study to analyse the post-injection migration of CO₂ plume into a dipping storage aquifer exposed to background flux velocity, including both residual trapping of CO₂ and CO₂ dissolution in brine as principal means of immobilising the mobile CO₂.

In this work, the post-injection migration of the injected CO₂ is identified at two stages as the early post-injection and late post-injection periods. This analysis studies the impact of

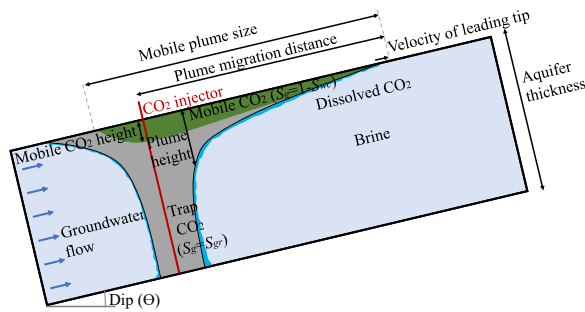


Fig. 1. Schematic diagram of CO₂ plume advancement in a tilted aquifer with background water flow during the early post-injection period. region 1 (green) contains mobile CO₂ and an irreducible brine saturation S_{wc} ; region 2 (grey) comprises mobile brine and a residual CO₂ saturation S_{gr} ; region 3 (blue) contains some dissolved CO₂ in brine.

the magnitude of groundwater flux on the early evolution of the injected CO₂ plume during post-injection period, and the importance of the residual trapping and dissolution of CO₂ in brine for plume migration. The study considered the density increase associated with the CO₂ dissolution in brine, but it suppresses the development of the convective mixing patterns due to the early timescale of the analysis and the relatively coarse gridding of the numerical model. We show that, in order to identify how fast and far the injected CO₂ plume travels during its early migration, and how much of it remains mobile before reaching the aquifer boundaries, it is very significant to evaluate the plume thickness, length and migrating velocity of its leading tip. Our next study focuses on the late post-injection migration of the CO₂ using a more refined gridding model and includes the convective dissolution of the injected CO₂ in brine.

The paper is organised as follows: first, we introduce the conceptual aquifer system and the questions addressed in this analysis. Secondly, we provide details of the aquifer model setup and the methodology developed for our study. This will then be followed by the main results and discussion of the findings.

2. Description of conceptual model

A schematic diagram of the aquifer model developed for this study is illustrated in Fig. 1. The supercritical CO₂ (green) is injected from a vertical well (red solid line) into an open tilted aquifer subjected to a background water flow (left to right in the diagram). The model considers residual trapping (grey) and CO₂ dissolution in brine (blue) during the post-injection period. Due to density differences between the injected CO₂ plume and brine, the injected plume of CO₂ will migrate upwards displacing the brine downwards. A portion of the injected plume will become residually trapped (grey) and this and the remaining mobile CO₂ will dissolve gradually into the brine (blue) as the plume migrates up-dip.

The migration of the injected plume of CO₂ in the aquifer occurs during injection and post-injection periods. In this study, we divide the post-injection migration of the plume into early post-injection and late post-injection periods. The

early post-injection migration is when some of the injected CO₂ is residually trapped and a fraction of the mobile plume dissolves in the contacted brine as it migrates; however, the dissolved front (blue) across the CO₂-brine interface in the migrating mobile plume region (green) does not reach the bottom boundary of the aquifer. The late post-injection migration of the plume is the period during which the CO₂ eventually stops migrating because it reaches a physical boundary, or its volume is exhausted by residual and dissolution trapping. Our main focus here is to capture the plume migration behaviour during the early post-injection period.

In this study, we are interested in investigating how fast and how far the injected CO₂ plume travels over time, and how much of it remains mobile during its early migration before reaching the system boundaries or a spill point. Understanding how the velocity of the background flow influences the CO₂ plume evolution in the aquifer during migration is important to tackle these questions. The numerical analysis will help in evaluating the plume distribution in the early post-injection period, which is essential for studying the migration of the injected plume, predicting the long-term fate of injected CO₂ plume, and identifying the risks of leakage of CO₂ to the surface in the late post-injection period-especially through abandoned wells, fractures or faults, which will be considered in our future work.

3. Numerical modelling approach

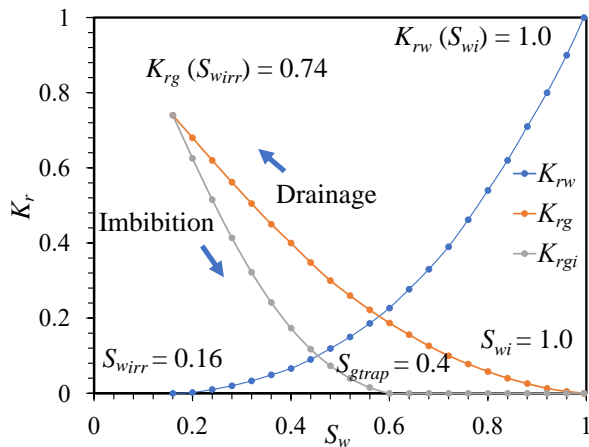
A synthetic aquifer model was constructed in the CMG-GEM simulator (CMG-GEM, 2022) based on the conceptual system provided in Fig. 1 to numerically analyse the impact of groundwater flow velocity on the CO₂ plume migration in a dipping aquifer system. CMG-GEM is a well-established, effective and multidimensional, equation-of-state (EOS) compositional simulator which was chosen from a variety of commercial simulators that can generate the same results (CMG-GEM, 2022). The major limitations of CMG-GEM as all other simulators are numerical and related to grid resolution and run time.

3.1 Methodology and model setup

A two-dimensional, homogenous, and isotropic model with uniform porosity and permeability is developed to understand the mechanisms associated with the subsurface migration and trapping of the injected CO₂ plume. Although aquifers are usually heterogeneous at some scale, the effect of heterogeneity on the plume evolution is beyond the scope of this study and will be considered in a separate study. Here, two fluids are modelled: brine as an aqueous defending phase and CO₂ as a supercritical displacing phase. The supercritical CO₂ properties including the density and viscosity are modelled with from the Peng and Robinson (1976) EOS and the Jossi et al. (1962) correlations, respectively. The aqueous phase is referred to as brine in this study although properties of pure water are assumed in the model. Brine composition is not included as we are interested in analysing the velocity of the background water rather than its composition, but we are aware of its significance on the aqueous phase properties and

Table 1. Aquifer model properties.

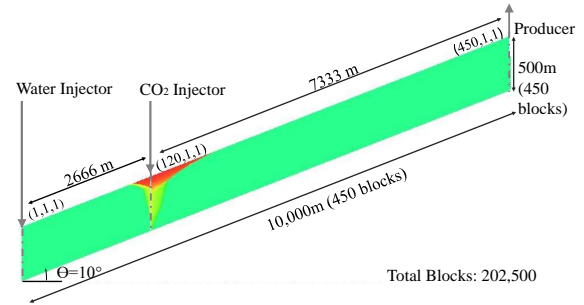
Model Parameters	Value
Length (m)	10,000
Number of grid blocks (I × J × K)	450 × 1 × 450
Porosity (%)	13
Horizontal Permeability K_h (mD)	97.5
Permeability anisotropy ratio (K_v/K_h)	1
Water viscosity (cp)	0.31
Water density (kg/m ³)	975
Reference depth to the top of the injector (m)	2,325
Initial reservoir pressure at top (kPa)	24,500
Reservoir temperature (°C)	95
Corey exponent for gas	1.8
Corey exponent for water	2.3

**Fig. 2.** Gas-water relative permeability functions used in this study.

hence on CO₂ trapping and migration. Rowe and Chou (1970) and Kestin et al. (1981) correlations are used to predict the density and viscosity of the aqueous phase, respectively. The study considers both isothermal calculations and the dissolution of CO₂ in the aqueous phase using Henry's law (Li and Nghiem, 1986; Harvey, 1996). However, geomechanical stresses or geochemical reactions, and water evaporation into the supercritical CO₂ are beyond the scope of this analysis. The aquifer is tilted with a positive dip angle of 10° and is initially saturated with water. The aquifer model has a fine grid resolution and a total pore volume of 6.5×10^9 m³, with the lateral dimension being 20 times the vertical dimension, to properly capture as much of the migration behaviour of the CO₂ plume before it reaches the aquifer boundaries. The aquifer parameters are shown in Table 1.

The relative permeability model used in this study is generated based on standard data set by CMG-GEM (2022) and shown in Fig. 2. CO₂ residual trapping in the wake of injected plume is modelled by including the relative perme-

ability hysteresis of the gas phase in the relative permeability

**Fig. 3.** Two dimensional representation of the aquifer model.

model. In this case, the hysteresis of the imbibition relative permeability curves is obtained with the Land (1968) correlation. In which, the residual CO₂ saturation was set to $S_{gr} = 0.4$ for the endpoint scenario where irreducible water saturation is reached during drainage. At this stage of analysis, the capillary pressure is not considered explicitly.

The aquifer includes, in addition to the modelled CO₂ injection well, a vertical water injection well and a vertical production well. The production well is at the up-dip side of the aquifer (at gridblock 450 in the I direction) and is perforated all the way through to simulate a constant pressure boundary condition, and allow for fluid (water and CO₂, if present) displacement from the aquifer as water is being injected. A two dimensional representation of the aquifer domain is shown in Fig. 3. The water injection well is located at the down-dip boundary (at gridblock 1 in the I direction) and is perforated all the way through the vertical interval to simulate a uniform background water flow across the aquifer thickness. The velocity of groundwater in aquifers is very slow relative to that at which pumped fluid flow, and less than 1 km/year Harter (2003). The groundwater flow velocities are reported as 0.01 to 0.1m/year in the Alberta basin in Canada (Bachu et al., 1994), and estimated as 0.04-0.4 m/year in an exemplar model based on Forties aquifer in the North Sea (Goater et al., 2013). Therefore, the background water in this analysis is assumed to flow from down-dip to up-dip with an average velocity of $U_w = 0.003048$ m/day (0.01 ft/day), which is enough to capture its effect on the plume migration and trapping in this modelling study. In a sensitivity study, the flow velocity (U_w) is varied from 0 to 15 U_w , to investigate its impact on the extent and height of the plume during migration (The flow velocity is held constant in each simulation run.).

The CO₂ injection well is located at gridblock 120 in the I direction, 2,666.7 m from the water injection well and perforated across the whole interval of the aquifer. Pure CO₂ is injected at a constant flow rate of 2.5% pore volume per year (equivalent to 307 kT/day) for a total duration of 1 year, followed by a shut-in period to analyse the plume migration and trapping in the dipping aquifer. The injection rate and period are selected to ensure the plume remained within the system boundaries during the total simulation run, for appropriate comparison in this conceptual study, and is a realistic rate. In reality, CO₂ may be injected for longer duration or at different injection rates.

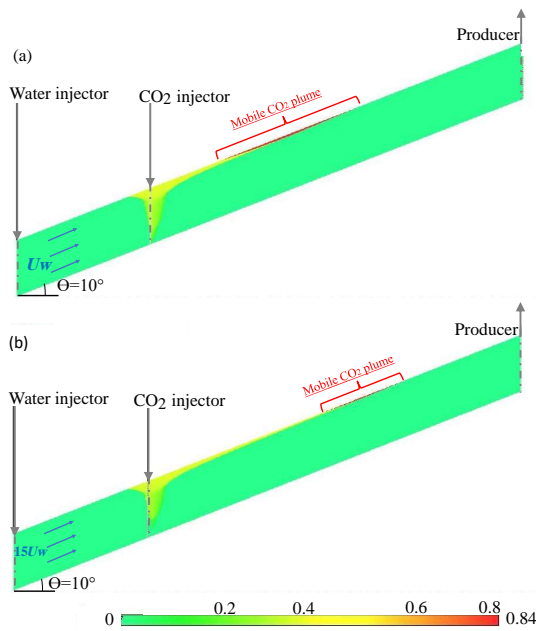


Fig. 4. Supercritical CO₂ phase saturation showing plume evolution profile after 20 years of simulation, for background water velocity flows of (a) $1 U_w$ and (b) $15 U_w$, respectively ($U_w = 0.003048$ m/day). The red and yellow regions of the plume show, respectively, mobile and immobile parts of the plume.

The simulations cease once the injected CO₂ plume reaches the up-dip boundary of the aquifer. This is identified based on the criteria of monitoring the production well with a surface gas production rate threshold of 1,000 m³/day. In all sensitivities performed in this study, the dissolved CO₂ at the leading tip of the plume reaches the up-dip boundary before the free phase CO₂ does. This is because as the plume migrates up-dip, its leading tip dissolves in the unsaturated brine and displaces the now CO₂ saturated brine ahead of the advancing supercritical CO₂ front. Hence, even though the supercritical CO₂ phase may be more mobile than the brine, dissolved CO₂ will always break through before the free phase CO₂ plume, which is an important aspect when downhole monitoring is considered.

In this numerical analysis, we study the impact of the velocity of background flux on the distribution, extent and velocity of the injected CO₂ plume during the early post-injection period. A post-processing MicroSoft Excel script with macro is developed to process the numerical results and give precise location of the plume at particular timesteps. A threshold critical gas saturation value of 0.005 is used in the script to specify the shape and extent of the CO₂ plume, including the mobile and residually trapped portions of the plume. A threshold relative permeability value of 0.01 is used in the script to obtain the shape and size of the mobile portion of the plume.

4. Results

Fig. 4 demonstrates the simulated distribution of the injected plume of CO₂ in the model setup shown in Fig. 3 after 20 years of simulation for background water velocity flows of

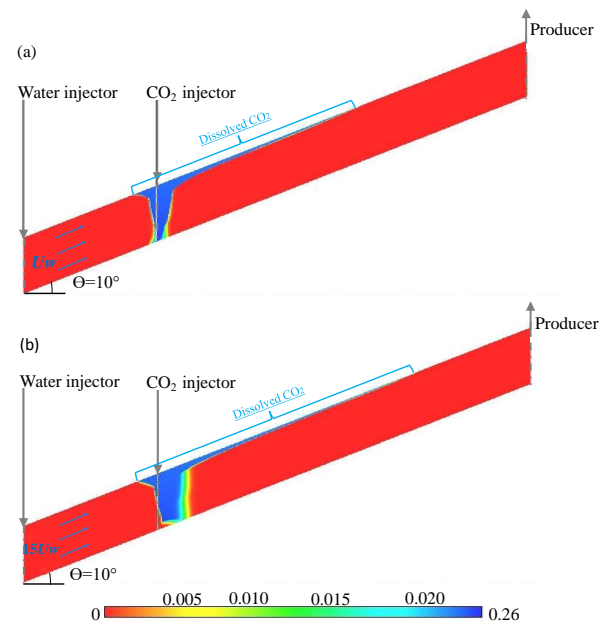


Fig. 5. Plume dissolution profile after 20 years of simulation, for background water velocities of (a) $1 U_w$ and (b) $15 U_w$, respectively ($U_w = 0.003048$ m/day). The red and blue regions of the plume show, respectively, the unsaturated brine and CO₂-saturated brine.

1 and $15 U_w$, respectively. As can be seen, due to the density difference between the injected CO₂ and the resident brine, the buoyant CO₂ plume migrates upwards from the injection point displacing the brine downwards, and then it propagates laterally along the top of the aquifer. The mobile CO₂ plume (the red portion in Fig. 4) continues to migrate leaving a trail of residually trapped CO₂ behind (the yellow portion in Fig. 4) due to the relative permeability hysteresis effect considered in the model. As can be observed from both profiles, the distribution of residually trapped CO₂ and mobile CO₂ within the injected plume differs with the background flow velocity.

Fig. 5 shows profiles of CO₂ plume dissolution in brine after 20 years of simulation for background flow velocity ratios of 1 and $15 U_w$, respectively – for the equivalent simulations and times as the phase saturations in Fig. 4. During the early migration of the buoyant CO₂ plume (the blue regions), CO₂ dissolves gradually into the brine, developing a denser diffusive boundary layer of CO₂-saturated brine at the CO₂ and brine interface (the green and yellow parts) than the unsaturated brine (the red region). As can be observed, the velocity of background water flow affects the CO₂-saturated brine boundary generation. The boundary layer of dissolved CO₂ increases in extent as background flow increases. In addition, the greater the velocity of fresh background water, the greater the dissolution of the mobile and of the residually trapped CO₂ around the injection well, and the further the CO₂ (both mobile and dissolved) moves up-dip.

The above results suggest that the background flow velocity can affect the CO₂ plume migration during the early post-injection period. Thus, in this study we investigate its impact on: (1) the distribution of the total injected plume (considering both the trapped and mobile portions of the injected plume)

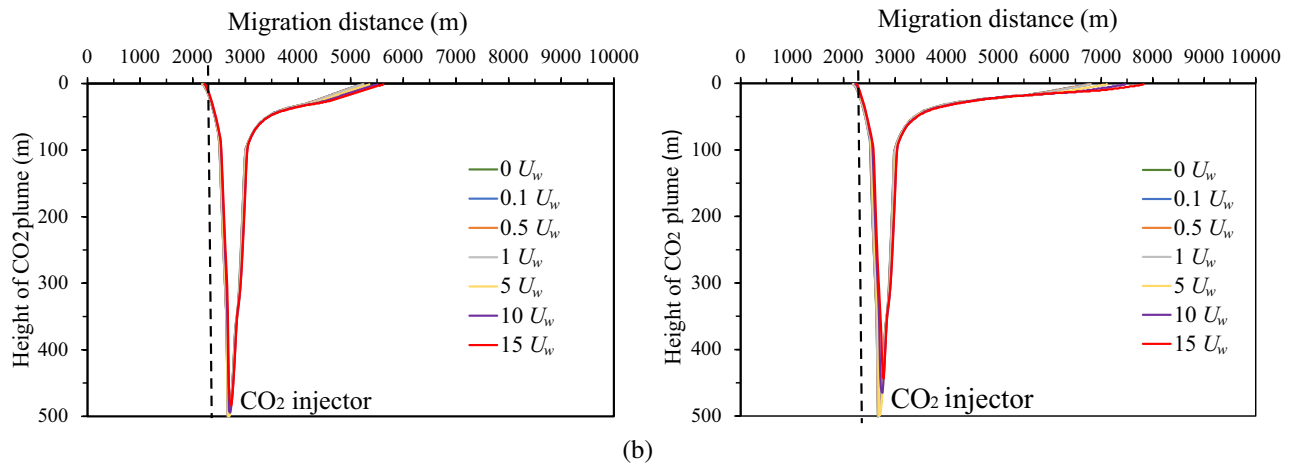


Fig. 6. Impact of background water velocity on the evolution of the CO₂ plume and migration distance after (a) 10 and (b) 20 years of simulation times.

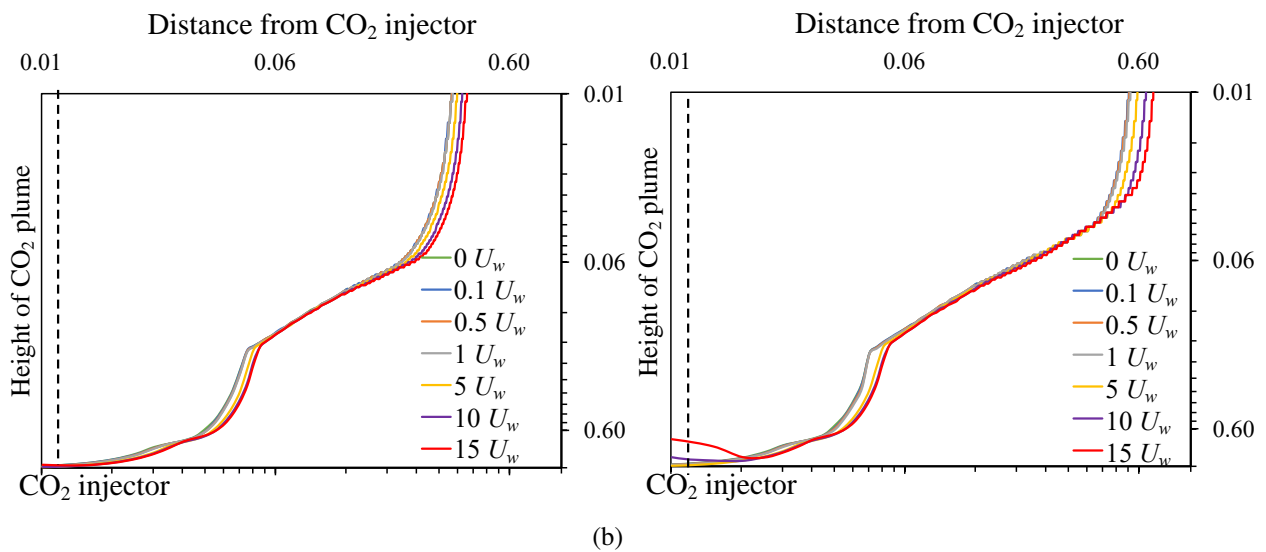


Fig. 7. Shows on logarithmic scale the dimensionless height of the entire CO₂ plume and migration distance from the injection well at different background flow velocities after (a) 10 and (b) 20 years of simulation times.

and (2) the distribution of the mobile CO₂ region of the plume, and (3) the instantaneous velocity of the tip of the plume as follows.

4.1 Background flow velocity effect on the CO₂ plume evolution

We consider the migration and spread of the injected CO₂ plume into the storage aquifer system described in the schematic diagram shown in Fig. 1 and the numerical results presented in Fig. 4 above. We first study the effect of the background flow velocity on the distribution and extent of the entire injected CO₂ plume, including both the mobile CO₂ and the residually trapped CO₂ within the plume (the red and yellow portions shown in Fig. 4, respectively). The following results of the distribution and extent of the injected CO₂ plume were both determined using the spreadsheet post-processing

module explained previously. Fig. 6 presents on a linear scale, the height and extent of the injected CO₂ plume at different background flow rates after 10 and 20 years of simulation. At greater background water velocities, the leading tip of the injected plume migrates further distances up-dip, whereas the plume height near the injection point decreases to some extent.

In order to precisely analyse the impact of background flux velocity on the plume distribution near the injection well, logarithmic scale plots of Fig. 6 are also considered in dimensionless form. Fig. 7 present the CO₂ plume height distribution versus migration distance from the injection well at different background velocity rates and times. Here, it is obvious that the height distribution of the injected plume changes and simultaneously decreases with time as the background flow velocity increases.

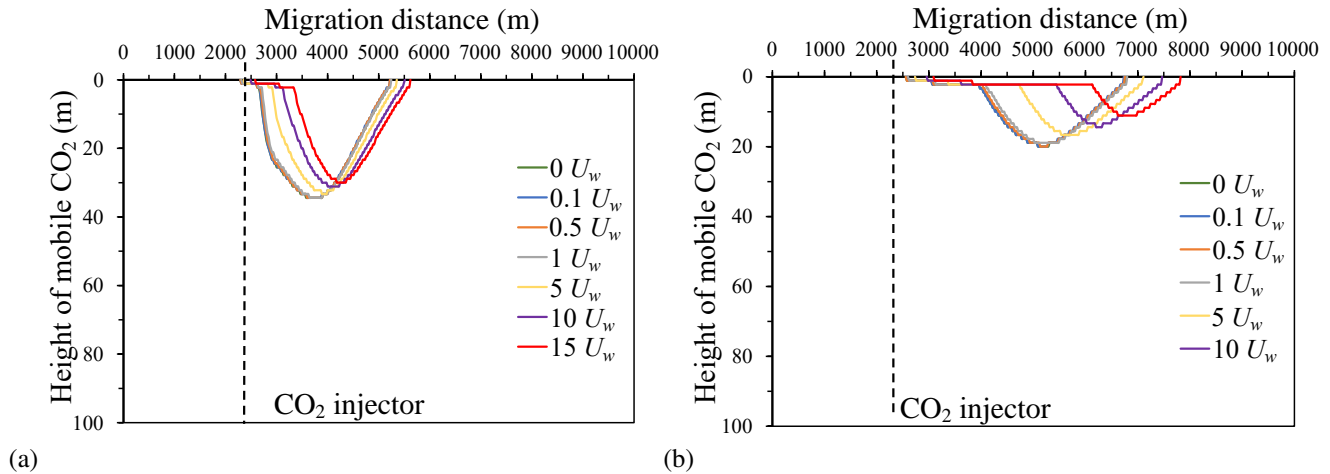


Fig. 8. Impact of background flow velocity ($U_w = 0.003048$ m/day) on the height and migration distance of the mobile CO_2 within the plume after (a) 10 and (b) 20 years of simulation times.

4.2 Background flow velocity effect on the migration of the mobile CO_2 within the plume

To understand the influence of background flux velocity on the plume distribution, its effect on the migration of the mobile portion of CO_2 within the plume was also considered. Fig. 8 illustrates the height and extent of the mobile CO_2 within the plume for different background flow velocities after 10 and 20 years of migration, respectively. Here, the spreadsheet script is used to obtain the exact location of the mobile CO_2 within the total injected plume in the storage aquifer. As can be seen in Fig. 8, both the upper and lower portions of mobile CO_2 migrated up-dip and its overall height diminished with time for greater background flow velocities.

Accurate assessment of the extent of the mobile CO_2 within the plume during its early migration is crucial since the leakage risk can be high in the short term. Table 2 shows the size or length of the mobile CO_2 under the top of the aquifer from its leading tip to its end at the lower portion, estimated at different water velocities. Fig. 9 presents the greatest height of the mobile CO_2 for different background flow velocities at different times. The results in Table 2 and Fig. 9 imply that the mobile CO_2 plume grows in size along the top of the aquifer, while its greatest depth reduces at greater background flow velocities. The reduction in thickness is most marked during the first four to five year after cessation of injection, as the bottom of the plume rises vertically, and the plume thickness reduces to less than 10% of its original thickness (the injection well being completed over the entire 500 m thickness of the aquifer).

During the post-injection evolution of the injected plume of CO_2 , several trapping mechanisms contribute to the reduction in volume of mobile CO_2 . Fig. 10 illustrates the inventory profiles of the injected CO_2 plume at low and high background flow velocities after 20 years of simulation. The volume of mobile CO_2 immobilised residually and particularly by dissolution in brine increased with flow velocity and with time.

Table 2. The length of mobile portion of the CO_2 plume from tip to its end at lowest portion for different background flow velocities.

Groundwater velocity ($U_w = 0.003048$ m/d)	Time	
	10 years	20 years
	Mobile CO_2 size (tail to tip) (m)	
$0 U_w$	2,911	4,178
$0.1 U_w$	2,889	4,111
$0.5 U_w$	2,889	4,156
$1 U_w$	2,889	4,156
$5 U_w$	2,956	4,333
$10 U_w$	2,978	4,467
$15 U_w$	3,000	4,689

4.3 Migration velocity of the leading tip of CO_2 plume

Assessing the migration velocity of the leading tip of the plume is crucial to analyse the advancement of the injected plume of CO_2 in the aquifer, which is important when addressing CO_2 storage security. Fig. 11 shows the instantaneous velocity of the CO_2 plume during the early post-injection period at different background velocities. The CO_2 plume decelerates with time during the very early post-injection migration, but then accelerates with time and with background flow velocity.

5. Discussion

The numerical results demonstrated in Figs. 4 and 5 show that, irrespective of the background water flow velocities, due to the tilt in the storage aquifer, the total distribution of the injected plume around the injection well is always asymmetr-

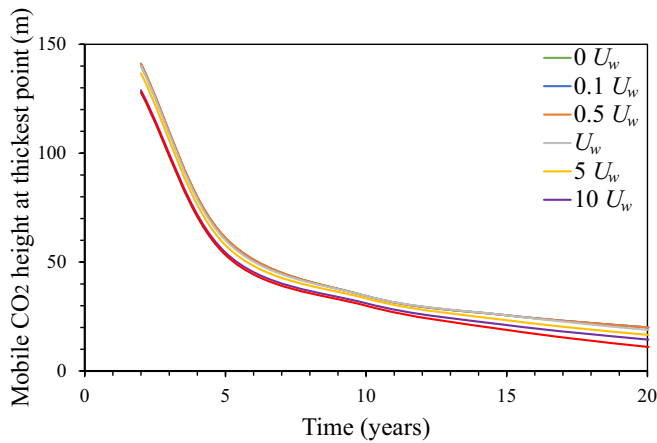


Fig. 9. presents the maximum height of the mobile CO₂ within the plume for different background flow velocity ($U_w = 0.003048$ m/d) and at different simulation times.

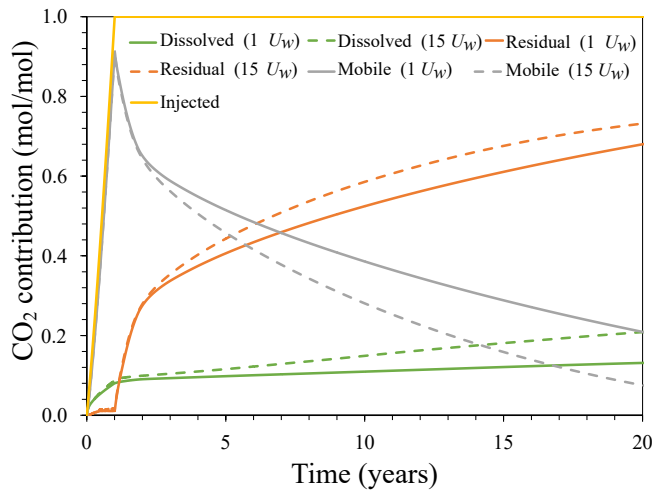


Fig. 10. Fate of CO₂ for background velocities of $1 U_w$ and $15 U_w$ ($U_w = 0.003048$ m/d) over time. The vertical axis represents the volume of CO₂ in each category in the inventory normalised relative to the total volume injected during the simulation.

ical. During the post-injection period, the less dense injected plume initially migrates upwards to the top boundary of the aquifer. The leading tip of the plume then migrates up-dip under buoyancy forces, but also moving with the groundwater flow, and propagates further with time. The lower end of the plume initially migrates down-dip due to viscous forces during injection; however, it only reaches a relatively short distance and then its flow direction reverses. In addition, comparison of the profiles, shown in Fig. 6, indicates that the plume extends with time, especially on the up-dip side, for the different flow velocities.

As can be seen in Fig. 6, the migration distance of the plume from the injection well increases as the plume migrates up-dip more quickly with increasing background flow velocity. This is more apparent at the leading tip of the plume, after 20 years (7.9 km for background velocity ratio $15 U_w$ compared to 6.6 km for background velocity ratio of $1 U_w$). This is because

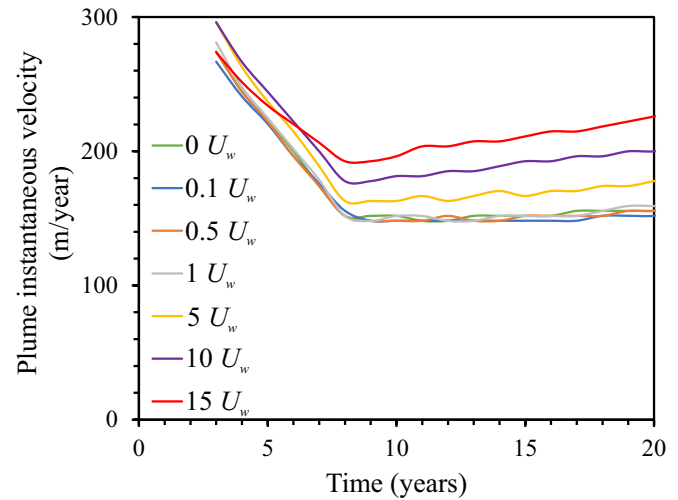


Fig. 11. Plume instantaneous velocity at different background flow velocities ($U_w = 0.003048$ m).

the background water flow increases the CO₂ plume lateral migration since both fluids flow in the same direction, thus causing the CO₂ to migrate larger distances. The difference in the plume height distribution with groundwater velocity is not evident on a linear scale. However, comparison of the logarithmic scale profiles shown in Fig. 7 indicates that as the velocity of groundwater flux increases the CO₂ plume height near the injection well decreases (The difference in the plume height can reach up to, approximately, 50 m between background flow velocities of $15 U_w$ and $1 U_w$ after 20 years of simulation). This is due to buoyancy effects and because the background flow displaces the CO₂ plume upwards due to the viscous pressure gradient. Our numerical analysis of the plume migration in dipping aquifers Awag (2022) and Juanes and MacMinn (2008) study of the plume migration in horizontal aquifers indicated that, the height of the total injected plume remains constant over time due to the residual CO₂ being immobile, although groundwater flow is modelled in these studies. In contrast to previous findings, our results here show that, although brine displaces CO₂ at the trailing edge leaving residually trapped CO₂ behind, as the unsaturated background water flow interacts with the plume it can also dissolve the CO₂, whether it was mobile or residually trapped, during the early migration of the plume. The rate of dissolution is greater at higher background water flow velocities, which is in line with the results of the analytical solution given by Emami-Meybodi et al. (2015). This is due to the greater mass of unsaturated brine that contacts the free phase CO₂, and thus the reduction in plume height near the injection well is more noticeable. This increase in dissolution of CO₂ at higher brine velocities, particularly at the tail of the plume, with the newly saturated brine then moving up-dip underneath the CO₂ plume, also reduces the extent to which the leading tip of the plume will come into contact with unsaturated brine. This will result in a reduction in the extent to which dissolution of CO₂ towards the leading edge of the plume retards the migration of the plume.

The profiles of the total distribution of the injected plume in

Fig. 6, compared to that of the mobile portion of CO₂ within the plume in Fig. 8, indicate that the effect of background flow on the distribution of the mobile CO₂ in the storage aquifer is important. As the mobile CO₂ migrates upwards, its leading tip travels larger distances, while its height decreases significantly with time as the background flow increases. This is due to the combined effect of the flow velocity and gravity force. During the early post-injection migration of the injected CO₂ plume, the upward flow of the mobile CO₂ is controlled by its density differences with the brine. However, the up-dip migration is increased, especially at the leading tip, because the presence of groundwater flow strengthens the upward displacement of the mobile CO₂ due to the viscous and the dissolution effects discussed above. Also, the reduction of the mobile CO₂ height within the plume is due to the enhanced retardation of CO₂ by residual trapping and dissolution with increasing the background flow velocity.

Inspection of the profiles in Fig. 8 identifies that the mobile CO₂ at the leading tip of the plume migrates upwards faster than the trailing end of the plume, lengthening the plume over time (as confirmed in Table 2). This is because, for any given saturation, CO₂ mobility is higher during drainage (the situation at the tip of the plume) than it is during imbibition (the situation at the trailing edge of the plume). Furthermore, as the plume elongates, the buoyancy force driving plume migration increases. As mentioned earlier, the leading tip of the plume is in continuous contact with unsaturated brine, and the resulting CO₂ dissolution will retard the plume progress somewhat. This retardation will be diminished at higher brine drift velocities, partially because of the viscous force associated with the brine flux, but also because the greater the brine flux, the more CO₂ saturated brine there will be towards the leading edge of the migrating plume, and so the less CO₂ dissolution in this location. By contrast, the trail of residually trapped CO₂ that is left behind during the imbibition process reduces the mobility of the brine that is contacting the mobile CO₂ and increases the resistance to water flow in the down-dip side, as confirmed by Juanes and MacMinn (2008). The slow migration of the lower side of mobile CO₂ results in a long tail of mobile CO₂; however, this is very narrow and becomes increasingly elongated at higher brine velocities.

The higher drift flux thus decreases the potential of CO₂ leakage through the injection well, but it increases the risk of the plume encountering a spill point feature or the storage boundaries earlier due to its faster up-dip migration. On the other hand, analysing this effect more closely from the profiles in Fig. 8, it is evident that the greater the velocity of background flow the thinner the mobile CO₂ plume becomes, particularly near the injection well, hence the less the volume of mobile CO₂ that can potentially leak to the surface should the plume encounter a leak point, or should the injection well itself leak post cessation of injection.

Table 2 and Fig. 9 support the above discussions. The results in Table 2 shows an extension in the length of the mobile CO₂ within the injected plume over time, but also an increase in the flow velocity accentuates this effect, due to the faster displacement of the leading tip of the plume as it travels up-dip. The difference in the length of mobile

CO₂ at the top of the aquifer can reach up to 500 meters between background velocities of 1 and 15 U_w after 20 years. However, as illustrated in Fig. 9, the height of mobile CO₂ at its maximum thickness decreased somewhat as the velocity of the groundwater increased (a maximum height of 10 meters compared to 20 meters after 20 years for flow velocities of 15 and 1 U_w , respectively). The reduction in mobile CO₂ thickness is due to the increase in the trapping of CO₂ as it migrates.

This can be further confirmed from the inventory profiles shown in Fig. 10, which compares the fate of injected CO₂ at low and high background flow velocities (1 and 15 U_w) after 20 years of migration. Increasing the background flow velocity exerts a great impact on reducing the volume of mobile CO₂ as it accelerates the residual trapping of CO₂ and, more significantly, enhances the dissolution of CO₂ in brine. The volume of mobile CO₂ decreased in this example from 21% to 7% with increase in the velocity of the groundwater flow from 1 to 15 U_w . While the background flow velocity and aquifer dip work together in speeding up the migration of the leading tip of the plume up-dip, as verified by MacMinn et al. (2010), this extends the contact surface area, allowing more CO₂ to interact with brine at the interface between the free-phase CO₂ and brine, hence increasing the CO₂ dissolution.

To understand the impact of the groundwater flow velocity on how fast the plume travels with time, we determined its effect on the migration velocity of the leading tip at small time intervals shown in Fig. 11. Inspection of the profiles in Fig. 11 shows that the plume initially decelerates with time until 8 years into the simulation in this case—irrespective of the magnitude of the background brine flow velocity. This begins after cessation of injection as the bottom of the plume rises vertically towards the caprock due to gravity. During this period there is a loss of mobile CO₂ at the trailing and bottom edges due to water imbibition and residual trapping, all the way from the bottom of the completion; this in turn slows down the plume vertical migration. The rapid deceleration stops when the slower lateral migration restricts the faster vertical buoyancy rise, and the plume continues to thin, but at a lower rate. At this time the plume geometry becomes dominated by its migration in the direction of flow, which is a consequence of the balance between buoyancy and viscous forces on the one hand, and trapping mechanisms on the other. The instantaneous velocity of the plume then increases with time, the more so for higher background flow velocities. This is due to the increasing buoyancy force as the plume becomes extended, its leading tip travelling faster than the trailing edge.

6. Conclusions

In this study, we investigate the impact the velocity of background flow has on the evolution and migration of an injected plume of CO₂ in a tilted storage aquifer by performing numerical simulation analysis. Our analysis focuses on the early migration of the injected CO₂ plume, giving estimates of the height, extent and velocity of the plume in addition to the volume of mobile CO₂ that remains in the system. Our results show that:

- 1) Regardless of the background water flow, the initial distribution of the total injected plume around the injection well is asymmetrical due to the impact of aquifer dip angle. However, increased water flow velocity extends the plume extent at the up-dip side, impacts the migration of the plume at the down-dip side and affects the eventual residual and dissolution trapping of the free phase CO₂.
- 2) The first thing that will be observed as the CO₂ plume approaches is not free phase CO₂, but CO₂ dissolved in water (perhaps detected as a change in pH). This is because CO₂ will dissolve into water at the leading tip of the plume, but then some of this now saturated water will be displaced ahead of the plume.
- 3) Increasing the background flow velocity increases the CO₂ migration distance at the leading tip of the injected plume, whereas it decreases its height near the injection well with time. The background water flow promotes the up-dip displacement of the injected CO₂ plume owing to the displacement of CO₂ saturated brine along with the buoyancy driven plume migration. The presence of a greater volume of saturated brine when the drift flux velocity is greater means less CO₂ can be dissolved into brine towards the tip (the brine being already saturated), and so less retardation of CO₂ due to dissolution.
- 4) The greater the background flow velocity the faster the up-dip migration of the mobile CO₂ at its leading tip compared with its lower portion. At the down-dip side the background flow is affected by the residually trapped CO₂, as it resists the flow. Furthermore, the height distribution of the mobile CO₂ decreases with time at higher background brine velocities because the background flow decreases the mobile CO₂ in the system by increasing its residual and dissolution trapping. Thus, at higher drift velocities the plume will migrate further, increasing the risk of the plume reaching a spill or leak point, but the volume of mobile CO₂ reduces significantly, reducing the amount of CO₂ that could potentially leak. Additionally, the risk of leakage at the injection well after cessation of injection will be significantly reduced. This is important, as an injection well represents a potential pathway to surface, albeit one that will have been carefully plugged and abandoned.
- 5) Our estimates of the migration velocity indicate that the plume initially decelerates with time, irrespective of the background flow velocity, because of the decrease in mobile CO₂ plume size due to trapping during its vertical upwards migration. The plume then accelerates with time during its lateral up-dip migration as the plume extends and thus buoyancy increases; this effect is greater at higher brine flow velocities due to the greater stretching of the plume.

In another study, we aim to study the impact of background water flow on the late post-injection evolution and migration of an injected plume of CO₂ as the plume eventually shrinks due to the dominance of the trapping mechanisms. Additionally, we will assess the volume of CO₂ that can be injected, whilst ensuring the plume is completely consumed before it reaches

the system boundaries or a spill point.

Acknowledgements

The Libyan Ministry of Education are thanked for sponsoring Mawda Awag. CMG are thanked for use of the GEM reservoir simulation software in this research. Energi Simulation are thanked for supporting the Chair in CCUS and Reactive Flow Simulation held by Eric Mackay.

Conflict of interest

The authors declare no competing interest.

Open Access This article is distributed under the terms and conditions of the Creative Commons Attribution (CC BY-NC-ND) license, which permits unrestricted use, distribution, and reproduction in any medium, provided the original work is properly cited.

References

- Awag, M., Mackay, E., Ghanbari, S. CO₂ plume migration in tilted aquifers subject to groundwater flow. Paper Presented at 83rd EAGE Annual Conference and Exhibition, Madrid, Spain, 1-5 June, 2022.
- Bachu, S. CO₂ storage in geological media: Role, means, status and barriers to deployment. *Progress in Energy and Combustion Science*, 2008, 34(2): 254-273.
- Bachu, S., Gunter, W., Perkins, E. Aquifer disposal of CO₂: Hydrodynamic and mineral trapping. *Energy Conversion and Management*, 1994, 35(4): 269-279.
- Bennaceur, K. CO₂ Capture and Sequestration, in *Future Energy (2nd)*, edited by T. M. Letcher, Elsevier, pp. 583-611. 2014.
- Benson, S. M., Cole, D. R. CO₂ sequestration in deep sedimentary formations. *Elements*, 2008, 4(5): 325-331.
- Birkholzer, J. T., Oldenburg, C. M., Zhou, Q. CO₂ migration and pressure evolution in deep saline aquifers. *International Journal of Greenhouse Gas Control*, 2008, 40: 203-220.
- CMG-GEM. Computer Modelling Group, 2022.
- Elenius, M., Voskov, D., Tchelepi, H. Interactions between gravity currents and convective dissolution. *Advances in Water Resources*, 2015, 83: 77-88.
- Emami-Meybodi, H., Hassanzadeh, H., Ennis-King J. CO₂ dissolution in the presence of background flow of deep saline aquifers. *Water Resources Research*, 2015, 51(4): 2595-2615.
- Goater, A. L., Bijeljic, B., Blunt, M. J. Dipping open aquifers—the effect of top-surface topography and heterogeneity on CO₂ storage efficiency. *International Journal of Greenhouse Gas Control*, 2013, 17: 318-331.
- Gunter, W., Wiwchar, B., Perkins, E. Aquifer disposal of CO₂-rich greenhouse gases: Extension of the time scale of experiment for CO₂-sequestering reactions by geochemical modelling. *Mineralogy and Petrology*, 1997, 59: 121-140.
- Han, W. S., Kue-Young, K., Esser, R. P., et al. Sensitivity study of simulation parameters controlling CO₂ trapping mechanisms in saline formations. *Transport in Porous Media*, 2011, 90: 807-829.
- Harter, T. Basic concepts of groundwater hydrology. California

- nia, University of California, 2003.
- Harvey, A. H. Semiempirical correlation for Henry's constants over large temperature ranges. *AIChE Journal*, 1996, 42(5): 1491-1494.
- Hassanzadeh, H., Pooladi-Darvish, M., Keith, D. The effect of natural flow of aquifers and associated dispersion on the onset of buoyancy-driven convection in a saturated porous medium. *AIChE Journal*, 2009, 55(2): 475-485.
- Hesse, M., Orr, F., Tchelepi, H. Gravity currents with residual trapping. *Journal of Fluid Mechanics*, 2008, 611: 35-60.
- Hesse, M., Tchelepi, H., Cantwel, B., Orr, F. Gravity currents in horizontal porous layers: transition from early to late self-similarity. *Journal of Fluid Mechanics*, 2007, 577: 363-383.
- Hesse, M. A., Tchelepi, H. A., Orr Jr, F. M. Scaling analysis of the migration of CO₂ in saline aquifers. Paper SPE 102796 Presented at SPE Annual Technical Conference and Exhibition, San Antonio, Texas, 24-27 September, 2006.
- Iglauer, S. Dissolution trapping of carbon dioxide in reservoir formation brine-A carbon storage mechanism, in *Mass Transfer-Advanced Aspects*, edited by H. Nakajima, In-Tech, pp. 233-262, 2011.
- IPCC. IPCC special report on carbon dioxide capture and storage. Prepared by Working Group III of the Intergovernmental Panel on Climate Change., Cambridge, United Kingdom and New York, Cambridge University Press, 2005.
- Jossi, J. A., Stiel, L. I., Thodos, G. The viscosity of pure substances in the dense gaseous and liquid phase. *AIChE J*, 1962, 8(1): 59-63.
- Juanes, R., MacMinn, C. W. Upscaling of capillary trapping under gravity override: Application to CO₂ sequestration in Aquifers. Paper SPE 113496 Presented at SPE Symposium on Improved Oil Recovery. Tulsa, Oklahoma, 20-23 April, 2008.
- Juanes, R., MacMinn, C. W., Szulczewski, M. L. The footprint of the CO₂ plume during carbon dioxide storage in saline aquifers: Storage efficiency for capillary trapping at the basin scale. *Transport in Porous Media*, 2009, 82(1): 19-30.
- Kestin, J., Khalifa, H. E., Correia, R. J. Tables of the dynamic and kinematic viscosity of aqueous NaCl solutions in the temperature range 20-150 °C and the pressure range 0.1-35 MPa. *Journal of Physical and Chemical Reference Data*, 1981, 10(1): 71-88.
- Land, C.E. Calculation of imbibition relative permeability for two- and three-phase flow from rock properties. *Society of Petroleum Engineers Journal*, 1968, 8(2): 149-156.
- Li, Y. K., Nghiem, L. X. Phase Equilibria of Oil, Gas and Water/Brine Mixtures from a Cubic Equation of State and Henry's Law. *The Canadian Journal of Chemical Engineering*, 64(3): 486-496.
- MacMinn, C. W., Juanes, R. Post-injection spreading and trapping of CO₂ in saline aquifers: Impact of the plume shape at the end of injection. *Computational Geosciences*, 2009, 13(4): 483-491.
- MacMinn, C., Szulczewski, M., Juanes, R. CO₂ migration in saline aquifers. Part 1. Capillary trapping under slope and groundwater flow. *Journal of Fluid Mechanics*, 2010, 662: 329-351.
- Nordbotten, J. M., Celia, M. A. Similarity solutions for fluid injection into confined aquifers. *Journal of Fluid Mechanics*, 2006, 561: 307-327.
- Nordbotten, J., Celia, M., Bachu, S. Injection and storage of CO₂ in deep saline aquifers: Analytical solution for CO₂ plume evolution during injection. *Transport in Porous Media*, 2005, 58(3): 339-360.
- Oelkers, E., Gislason, S., Matter, J. Mineral carbonation of CO₂. *Elements*, 2008, 4: 333-337.
- Pawar, R., Chu, S., Makedonska, N., et al. Assessment of relationship between post-injection plume migration and leakage risks at geologic CO₂ storage site. *International Journal of Greenhouse Gas Control*, 2020, 101: 103138.
- Peng, D.Y. and Robinson, D.B. A new two-constant equation of state. *Industrial & Engineering Chemistry Fundamentals*, 1976, 15(1): 59-64.
- Pentland, C. H., El-Maghraby, R., Iglauer, S., et al. Measurements of the capillary trapping of super-critical carbon dioxide in Berea sandstone. *Geophysical Research Letters*, 2011, 38: 1-4.
- Pruess, K., Nordbotten, J. Numerical simulation studies of the long-term evolution of a CO₂ plume in a saline aquifer with a sloping caprock. *Transport in Porous Media*, 2011, 90: 135-151.
- Riaz, A., Cinar, Y. Carbon dioxide sequestration in saline formations: Part I-Review of the modeling of solubility trapping. *Journal of Petroleum Science and Engineering*, 2014, 124: 367-380.
- Rosenbauer, R. J., Thomas, B. Carbon dioxide (CO₂) sequestration in deep saline aquifers and formations, in *Developments and Innovation in Carbon Dioxide (CO₂) Capture and Storage Technology*, edited by M. M. Maroto-Valer. Woodhead Publishing, pp. 57-103, 2010.
- Rowe, A. M., Chou, J. C. Pressure-volume-temperature-concentration relation of aqueous sodium chloride solutions. *Journal of Chemical and Engineering Data*, 1970, 15(1): 61-66.
- Zhang, D., Song, J. Mechanisms for geological carbon sequestration. *Procedia IUTAM*, 2014, 10: 319-327.